Materials Physics and Mechanics 22 (2015) 125-135 Received: December 16, 2014

FREQUENCY ANALYSIS OF A GRAPHENE SHEET EMBEDDED IN AN ELASTIC MEDIUM WITH CONSIDERATION OF SMALL SCALE

A.T. Samaei[1*], M.R.M. Aliha[2], M.M. Mirsayar[3]

[1]University of California Merced, School of Engineering, University of California, Merced, CA 95343, USA

United States[2]Welding and Joining Research Center, School of Industrial Engineering, Iran University of Science and Technology, Narmak, 16846-13114, Tehran, Iran

[3]Zachry Department of Civil Engineering, Texas A&M University, College Station, TX 77843-3136, USA

*e-mail address: atourkisa2-c@my.cityu.edu.hk

Abstract. The effect of length scale on the vibration response of a single-layer graphene sheet embedded in an elastic medium is studied using nonlocal Mindlin plate theory. The elastic medium is modeled using both Winkler-type and Pasternak-type elastic foundations. An explicit solution is derived for the natural frequencies of the graphene sheet. Through the analytical solution it is found that the vibration response of graphene sheet concerning the length scale effects considerably different from the results obtained by the classical theories. In comparison with the classical plate theory, the nonlocal model showed that the natural frequency of the graphene sheet decreases for smaller lengths of graphene sheet, higher aspect ratios, greater values of nonlocal parameter and stiffer elastic foundations.

Nomenclature

a	material constant depending on the internal length (nm),
b	graphene sheet width (nm),
e_0	calibrating constant suitable to each material,
h	graphene sheet thickness (nm),
l	graphene sheet length (nm),
k_w, k_s	Winkler modulus, shear modulus of the surrounding elastic medium,
m	half wave number,
n	half wave number,
p	force per unit area,
t	time (s),
u, v	displacement of the point (x, y, 0) of graphene sheet along x and y-axis (nm),
w	deflection of the graphene sheet at point (x, y) calculated (nm),
C_{ijkl}	classical stress tensor,
D	bending rigidity of graphene sheet,
E	Young's modulus (N/m^2),
G	shear modulus (N/m^2),
M_{xx}, M_{yy}	resultant moments (Nm),
M_{xy}	twisting moment (Nm),
N_{xx}	in-plane force (N),
Q_x, Q_y	transverse shear forces (N),
ε_{kl}, ε_{xx}, ε_{yy}, ε_{xy}, ε_{xz}, ε_{yz}, ε_{zz}	linear strain tensor,
κ^2	transverse shear correction coefficient,
ν	Poisson's ratio,
ρ	mass density (kg/m^3),
σ_{ij}, σ_{xx}, σ_{yy}, σ_{xy}, σ_{xz}, σ_{yz}	nonlocal stress tensor (N/m^2),
τ	nonlocal parameter,

embedded in an elastic medium. As shown in Fig. 1, the graphene sheet is modeled as a moderately thick rectangular plate resting on two-parameter elastic foundation with the elastic modulus E, Poisson's ratio ν, uniform thickness h, length l and width b. A coordinate system (x, y, z) is also defined in Fig. 1 with x, y and z axes along the length, width and thickness of the graphene sheet, respectively.

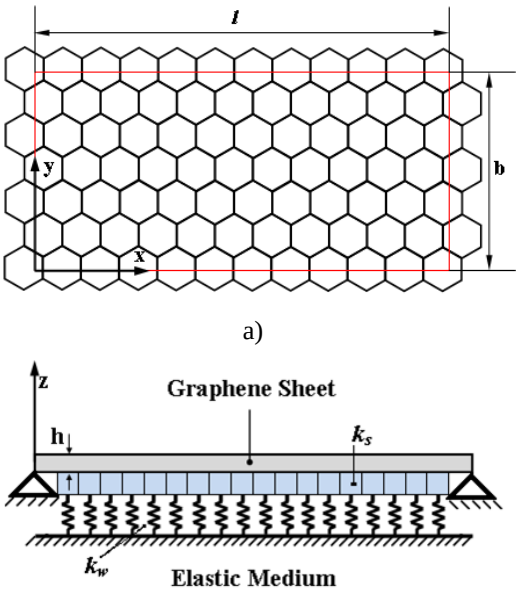

Fig. 1. Geometry of the considered graphene sheet embedded in elastic medium.

On the basis of the Mindlin plate theory, the governing differential equations of motion for the free vibration of the graphene sheet can be explained as follows [22]

$$M_{xx,x} + M_{xy,y} - Q_x = -\frac{1}{12}\rho h^3 \ddot{\psi}_x, \tag{1a}$$

$$M_{yy,y} + M_{xy,x} - Q_y = -\frac{1}{12}\rho h^3 \ddot{\psi}_y, \tag{1b}$$

$$Q_{x,x} + Q_{y,y} - p = \rho h \ddot{\psi}_z, \tag{1c}$$

where M_{xx} and M_{yy} are the resultant moments, M_{xy} is the twisting moment, and Q_x and Q_y are the transverse shear forces. All the aforementioned moments are per unit length. ψ_x and ψ_y are also the rotational displacements about y and x axes, respectively and ψ_z is the transverse displacement. In equation (1), t indicates also the time, ρ is the mass density and p is the force per unit area applied to the graphene sheet. It should be noted that in this paper, the symbol "," is used to show derivative operator. For example, $M_{xy,x}$ is equal to $\partial M_{xy}/\partial x$. Nonlocal elasticity theory states that the stress at each point in an elastic continuum medium depends not only on the strain of the same point but also on the strains at all other points in the domain [13, 14]. The nonlocal constitutive equations for a three-dimensional problem can be expressed as

$$(1 - \tau^2 l^2 \nabla^2)\sigma_{ij} = C_{ijkl}\varepsilon_{kl}, \tag{2}$$

where $\nabla^2, \sigma_{ij}, C_{ijkl}$ and ε_{kl} are the Laplacian operator, the stress tensor of the nonlocal elasticity, the classical stress tensor and the linear strain tensor, respectively. τ is also a material constant (called the nonlocal parameter) which depends on the internal length a [23] (such as the $C-C$ bond length, lattice parameter, granular size) and the external length l

where $D = Eh^3/12(1-\nu^2)$ is the bending rigidity of the graphene sheet. By ignoring the effect of nonlocal parameter (e_0a) in equations (6a) to (6e), the stress-resultant displacement relations will be identical to the relations obtained from the classical (or local) plate model. In addition, the in-plane edge load provides a force component for a deflected plate in transverse direction as:

$$p = N_{xx}\psi_{z,xx}, \tag{7}$$

where N_{xx} is the in-plane edge load per unit length. Consequently, by substituting equations (6a) to (6e) and (7) into equations (1a) to (1c), the governing differential equations of motion using nonlocal Mindlin plate theory are derived as follows:

$$\psi_{x,xx} + \psi_{x,yy} + \left(\frac{1+\nu}{1-\nu}\right)\left[\psi_{x,xx} + \psi_{y,xy}\right] - \left(\frac{2\kappa^2 Gh}{D(1-\nu)}\right)\left[\frac{\partial w}{\partial x} + \psi_x\right]$$
$$-\frac{1}{12}\rho h^3\psi_{x,tt} + \frac{(e_0a)^2}{12}\rho h^3\left[\psi_{x,xxtt} + \psi_{x,yytt}\right] = 0, \tag{8a}$$

$$\psi_{y,xx} + \psi_{y,yy} + \left(\frac{1+\nu}{1-\nu}\right)\left[\psi_{y,yy} + \psi_{x,xy}\right] - \left(\frac{2\kappa^2 Gh}{D(1-\nu)}\right)\left[\frac{\partial w}{\partial y} + \psi_y\right]$$
$$-\frac{1}{12}\rho h^3\psi_{y,tt} + \frac{(e_0a)^2}{12}\rho h^3\left[\psi_{y,xxtt} + \psi_{y,yytt}\right] = 0, \tag{8b}$$

$$\frac{\partial^2 w}{\partial x^2} + \frac{\partial^2 w}{\partial y^2} + \left[\psi_{x,x} + \psi_{y,y}\right] + N_{xx}\frac{\partial^2 w}{\partial x^2} + k_s\left[\frac{\partial^2 w}{\partial x^2} + \frac{\partial^2 w}{\partial y^2}\right]$$
$$-k_w w - \rho h\frac{\partial^2 w}{\partial t^2} + (e_0a)^2\rho h\left[\frac{\partial^4 w}{\partial x^2\partial t^2} + \frac{\partial^4 w}{\partial y^2\partial t^2}\right] - (e_0a)^2\left[N_{xx}\frac{\partial^4 w}{\partial x^4} + N_{xx}\frac{\partial^4 w}{\partial x^2\partial y^2} + \right.$$
$$\left. k_s\left[\frac{\partial^4 w}{\partial x^4} + \frac{\partial^4 w}{\partial y^4} + 2\frac{\partial^4 w}{\partial x^2\partial y^2} - k_w\left[\frac{\partial^2 w}{\partial x^2} + \frac{\partial^2 w}{\partial y^2}\right]\right]\right] = 0, \tag{8c}$$

where $k_s = K_s l^2/D$ and $k_w = K_w l^4/D$ are the dimensionless shear and Winkler foundation coefficients, respectively. It is worth mentioning that the aforementioned governing differential equations are reduced to those of the classical Mindlin plate model when the scale coefficient (e_0a) becomes equal to zero.

3. Solution using Navier's approach

In Navier's approach, the generalized displacement field is expanded in trigonometric series such that the boundary conditions of the problem are satisfied. In the following, the solution of governing differential equations obtained in previous section for the rectangular plates with simply supported boundary conditions is presented using Navier's method. The simply supported boundary conditions for the plate model are

$$w = 0,\ \psi_y = 0\ \ and\ \ M_{xx} = 0 \quad at\ \ x = 0, l \tag{9a}$$

$$w = 0,\ \psi_x = 0\ \ and\ \ M_{yy} = 0 \quad at\ \ y = 0, b \tag{9b}$$

The general form of expanded displacement components are assumed to be as

$$\psi_x = \sum_{m=1}^{\infty}\sum_{n=1}^{\infty}\Psi_{nm}\cos(\zeta_m x)\sin(\eta_n y)\sin\omega_{nm}t, \tag{10a}$$

$$\psi_y = \sum_{m=1}^{\infty}\sum_{n=1}^{\infty}\Phi_{nm}\sin(\zeta_m x)\cos(\eta_n y)\sin\omega_{nm}t, \tag{10b}$$

$$w = \sum_{m=1}^{\infty}\sum_{n=1}^{\infty}W_{nm}\sin(\zeta_m x)\sin(\eta_n y)\sin\omega_{nm}t, \tag{10c}$$

where Ψ_{nm}, Φ_{nm} and W_{nm} are constant coefficients and ζ_m and η_n are defined as $\zeta_m =$

4.2. Small scale effect on the frequency ratio of the graphene sheet. After verifying the accuracy of the present analytical solution, the following new results are presented for the graphene sheets under external in-plane loads and resting on elastic foundation. Figures 3 to 7 show the influence of scaling coefficient (e_0a), surrounding elastic medium (k_w and k_s), aspect ratio (l/b), length of graphene sheet (l) and the mode of vibration (m) on the frequency ratio of graphene sheet based on the nonlocal elasticity solutions. It can be demonstrated that by setting $e_0a = 0$ in the governing vibration equations of the nonlocal plate (i.e. equations (8a) to (8c)), the classical elastic plate vibration equations (presented by Hashemi *et al.* [24]) are obtained. In addition, by setting $D = EI$ and $b = 0$ in equations (8a) to (8c) the nonlocal solution for the free vibration of a beam is obtained that is consistent very well with the Reddy's results [26].

Figure 3 shows the variations of the frequency ratio of the graphene sheet (for the first natural mode) with plate length and for different values of the nonlocal parameter (e_0a). The nonlocal parameter was chosen between 0 to $2nm$ because according to Sudak [27], (e_0a) should be smaller than $2\,nm$ for single-walled carbon nanotubes. For plotting the curves of Fig. 3, Winkler and shear modulus parameters were considered to be constant and equal to $k_w = 250$ and $k_s = 0$, respectively and the modes of vibration were assumed as $m = 1$ and $n = 1$. As it is seen from Fig. 3, the length scale coefficient decreases the frequency ratio (i.e. the natural frequency of the graphene sheet). Moreover, according to this figure, while for the small lengths of the plate, the non-local parameter affects significantly the value of natural frequency, its influence becomes negligible for the larger plate lengths (typically $l \geq 20\,nm$). In addition when the nonlocal parameter increases, the natural frequencies of the nonlocal solutions become smaller than those of the classical solutions because of the negative sign of e_0a term in equations (8a) to (8c).

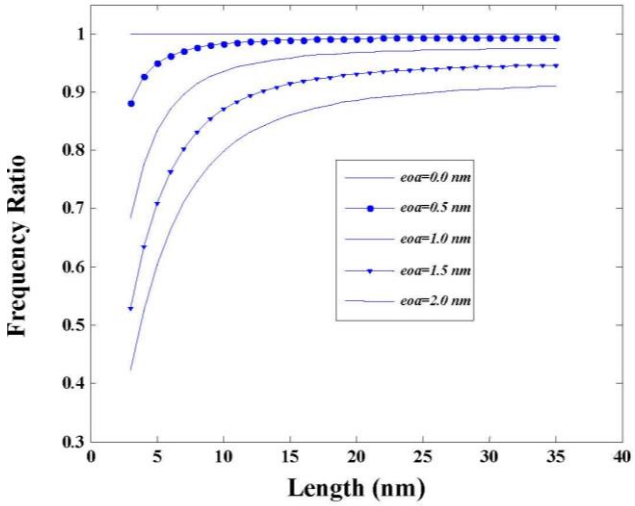

Fig. 3. Variations of frequency ratio with graphene sheet length (l) for different nonlocal parameters.

Figure 4 displays the variations of frequency ratio with the length of graphene sheet for different modes of vibration. It can be seen from Fig. 4 that for any given plate length, the corresponding value of natural frequency of the graphene sheet becomes smaller for the higher frequency mode numbers. The deference between the results of mode numbers increases by decreasing l showing the significant influence of nonlocal solution on the frequency response of graphene sheets having smaller plate lengths. Furthermore, at lower modes of vibration and for the higher lengths of plate all the results converge to the classical frequency of local plate [24] and the influences of small scale effects disappear.

Similarly, Fig. 6 illustrates also the effect of shear modulus parameter k_s on the frequency ratio of the graphene sheet in the presence of nonlocal parameter. The elastic medium was modeled as a Pasternak type foundation model with $k_w = 250$ and the shear modulus parameter was varied as follows: $k_s = 2, 4, 6, 8, 10$. These values for the shear modulus parameter (k_s) were also used by Liew *et al.* [28]. It can be seen that by increasing the shear modulus parameter of elastic medium the frequency ratio of graphene sheet resting on a Pasternak type model foundation decreases for any given nonlocal parameters. Again, reduction in the frequency ratio becomes more noticeable for the greater nonlocal parameters.

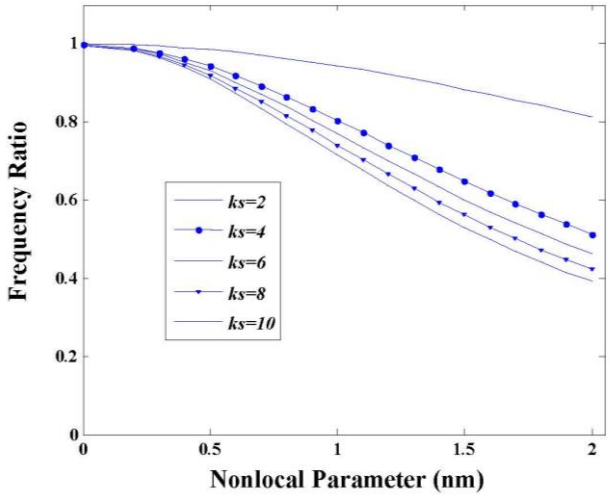

Fig. 6. Influence of small scale effects on the frequency ratio of graphene sheet for various shear modulus parameters k_s.

4.4. Effect of aspect ratio on the frequency ratio of the graphene sheet. The variation of the frequency ratio $(\omega_{nonlocal}/\omega_{local})$ versus the aspect ratio (l/b) for the considered rectangular Mindlin plate (graphene sheet) has been presented in Fig. 7 for different values of $e_0 a$. According to Fig. 7, the results obtained from nonlocal elastic solution are smaller than the corresponding results of the classical solution for the all aspect ratios. In addition the frequency ratio reduces by increasing l/b. It can be also seen that the length scale effects are more pronounced in vibration of rectangular graphene sheets than the strip-type graphene sheets (nanoribbons).

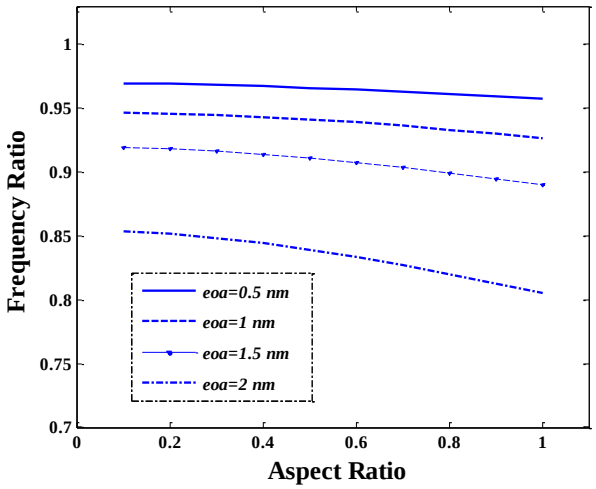

Fig. 7. Variations of frequency ratio with aspect ratio (l/b) for different nonlocal parameters,($m = 1, n = 1$).

5. Conclusions

- The vibration response of a single-layer graphene sheet embedded in an elastic medium was studied using nonlocal Mindlin plate theory.
- An explicit solution which takes into account the influence of length scale and surrounding elastic medium was derived for obtaining the natural frequencies of micro/nanoscaled Mindlin plates (such as graphene sheets).
- It was found that the effect of small scale is more pronounced for higher modes of vibration, greater Winkler and shear modulus parameters and larger length/width aspect ratios.
- The comprehensive model presented in this study provides useful results for vibration design aspects of NEMS devices such as graphene vibrators.

Appendix

Coefficients d_{11} through d_{33} are:

$$d_{11} = \zeta_m^2 + \eta_n^2 + \frac{2Ghk^2}{D(1-\upsilon)} + \frac{(1+\upsilon)}{(1-\upsilon)}\zeta_m^2 - \frac{1}{12}\rho h^3\omega_{nm}^2 - \frac{1}{12}\rho h^3\omega_{nm}^2(e_0a)^2(\zeta_m^2+\eta_n^2), \quad \text{(A.1)}$$

$$d_{12} = \zeta_m^2\eta_n^2\frac{(1+\upsilon)}{(1-\upsilon)}, \quad \text{(A.2)}$$

$$d_{13} = \frac{2Ghk^2}{D(1-\upsilon)}\zeta_m^2, \quad \text{(A.3)}$$

$$d_{21} = \zeta_m^2\eta_n^2\frac{(1+\upsilon)}{(1-\upsilon)}, \quad \text{(A.4)}$$

$$d_{22} = \zeta_m^2 + \eta_n^2 + \frac{2Ghk^2}{D(1-\upsilon)} + \frac{(1+\upsilon)}{(1-\upsilon)}\eta_n^2 - \frac{1}{12}\rho h^3\omega_{nm}^2 - \frac{1}{12}\rho h^3\omega_{nm}^2(e_0a)^2(\zeta_m^2+\eta_n^2), \quad \text{(A.5)}$$

$$d_{23} = \frac{2Ghk^2}{D(1-\upsilon)}\eta_n^2, \quad \text{(A.6)}$$

$$d_{31} = -\zeta_m^2, \quad \text{(A.7)}$$

$$d_{32} = -\eta_n^2, \quad \text{(A.8)}$$

$$d_{33} = -\zeta_m^2 - \eta_n^2 + \rho h\omega_{nm}^2 + \rho h\omega_{nm}^2(e_0a)^2(\zeta_m^2+\eta_n^2) - k_s$$
$$-\zeta_m^2N_{xx} - (e_0a)^2[k_w(\zeta_m^4+\eta_n^4+\zeta_m^2\eta_n^2) - k_s(\zeta_m^2-\eta_n^2) + \zeta_m^4N_{xx} + \zeta_m^2\eta_n^2N_{xx}]. \quad \text{(A.9)}$$

References

[1] S. Iijima // *Nature* **354 (6348)** (1991) 56.
[2] K. Esumi, M. Ishigami, A. Nakajima, K. Sawada, H. Honda // *Carbon* **34** (1996) 279.
[3] F. Scarpa, S. Adhikari, A. Srikantha Phani // *Nanotechnology* **20(6)** (2009) 065709.
[4] K. Tanaka, H. Aoki, H. Ago, T. Yamabe, K. Okahara // *Carbon* **35** (1997) 121.
[5] C. Berger, Z. Song, T. Li, X. Li, A.Y. Ogbazghi, R. Feng, Z. Dai, A.N. Marchenkov, E.H. Conrad, P.N. First, W.A. de Heer // *The Journal of Physical Chemistry B* **108(52)** (2004) 19912.
[6] J.S. Bunch, A.M. Van Der Zande, S.S. Verbridge, I.W. Frank, D.M. Tanenbaum, J.M. Parpia, H.G. Craighead, P.L. McEuen // *Science* **315** (2007) 490.
[7] C. Soldano, A. Mahmood, E. Dujardin // *Carbon* **48** (2010) 2127.
[8] A. Sakhaee-Pour, M.T. Ahmadian, A. Vafai // *Solid State Communications* **145** (2008) 168.
[9] K. Behfar, R. Naghdabadi // *Composites Science and Technology* **65(7-8)** (2005) 1159.
[10] A. Sakhaee-Pour, M.T. Ahmadian, R. Naghdabadi // *Nanotechnology* **19(8)** (2008) 085702.

[11] B.I. Yakobson, C.J. Brabec, J. Bernholc // *Physical Review Letters* **76** (1996) 2511.
[12] N.M. Ghoniem, E.P. Busso, N. Kioussis, H. Huang // *Philosophical Magazine* **83** (2003) 3475.
[13] A.C. Eringen, D.G.B. Edelen // *International Journal of Engineering Science* 10 (1972) 233.
[14] A.C. Eringen // *International Journal of Engineering Science* **10** (1972) 425.
[15] Sh.H. Hashemi, A.T. Samaei // *Physica E (Low-dimensional systems and nanostructures)* **43(7)** (2011) 1400.
[16] P. Lu, P.Q. Zhang, H.P. Lee, C.M. Wang, J.N. Reddy // *Proceedings of the Royal Society A* **463(2088)** (2007) 3225.
[17] W.H. Duan, C.M. Wang // *Nanotechnology* **18(38)** (2007) 385704.
[18] T. Murmu, S.C. Pradhan // *Journal of Applied Physics* **106** (2009) 104301.
[19] S.C. Pradhan, J.K. Phadikar // *Physics Letters A* **373(11)** (2009) 1062.
[20] A.T. Samaei, S. Abbasion, M.M. Mirsayar // *Mechanics Research Communications* **38(7)** (2011) 481.
[21] T. Murmu, S.C. Pradhan // *Journal of Applied Physics* **105** (2009) 064319.
[22] S. Timoshenko, S. Woinowsky-Krieger, *Theory of Plates and Shells* (McGraw-Hill, New York, 1959).
[23] R. Maranganti, P. Sharma // *Physical Review Letters* **98** (2007) 195504.
[24] Sh.H. Hashemi, K. Khorshidi, M. Amabili // *Journal of Sound and Vibration* 315 (2008) 318.
[25] W. Soedel, *Vibrations of Shells and Plates* (Marcel Dekker, New York, 1993).
[26] J.N. Reddy // *International Journal of Engineering Science* **45** (2007) 288.
[27] L.J. Sudak // *Journal of Applied Physics* **94** (2003) 7281.
[28] K.M. Liew, X.Q. He, S. Kitipornchai // *Acta Materialia* **54** (2006) 4229.
[29] M. Kim, H.S. An, W.-J. Lee, J. Jung // *Electronic Materials Letters* **9(4)** (2013) 517.
[30] M. Mazar Atabaki, R. Kovacevic // *Electronic Materials Letters* **9(2)** (2013) 133.
[31] W.G. Lee, E. Kim, J. Jung // *Electronic Materials Letters* **8(6)** (2012) 609.
[32] A. Ghorbanpour Arani, R. Kolahchi, H. Vossough // *Physica B: Condensed Matter* **407(22)** (2012) 4458.
[33] S. Adhikari, T. Murmu, M.A. McCarthy // *Finite Elements in Analysis and Design* **63** (2013) 42.
[34] Sh. Hosseini-Hashemi, M. Zare, R. Nazemnezhad // *Composite Structures* **100** (2013) 290.
[35] M. Sobhy // *Journal of Mechanics* **30(05)** (2014) 443.
[36] R. Ansari, A. Shahabodini, A. Alipour, H. Rouhi // *Proceedings of the Institution of Mechanical Engineers, Part N: Journal of Nanoengineering and Nanosystems* **226(2)** (2012) 51.
[37] M. Sobhy // *Physica E: Low-dimensional Systems and Nanostructures* **56** (2014) 400.
[38] M. Sobhy // *Acta Mechanica* **225** (2014) 2521.
[39] M. Heydari, A. H. Nabi, M. Heydari // *Nonlinear Dynamics* **78(3)** (2014) 1645.
[40] G. Allegri, F. Scarpa, R. Chowdhury, S. Adhikari // *Journal of Vibration and Acoustics* **135(4)** (2013) 041017.
[41] S. Sarrami-Foroushani, M. Azhari // *International Journal of Mechanical Sciences* **85** (2014) 168.
[42] S.A. Fazelzadeh, E. Ghavanloo // *Mechanics Research Communications* **56** (2014) 61.
[43] M. Sobhy // *International Journal of Mechanical Sciences* **90** (2015) 171.
[44] M.E. Golmakani, J. Rezatalab // *Composite Structures* **119** (2015) 238.